

THE ROLE OF A VARIABLE IMPULSE THRESHOLD IN THE IMPULSE FREQUENCY RESPONSE OF A TONIC SENSORY NEURON

JURGEN F. FOHLMEISTER*
*Department of Physiology, University of Minnesota,
Minneapolis, MN 55455, U.S.A.*

(Received August 25, 1981)

Abstract

Instantaneous threshold and a corresponding threshold potential are defined in terms of neural accommodation and membrane refractoriness whose actions are then evaluated in the context of low frequency repetitive firing of nerve impulses. The role of threshold variations as a part of the mechanism of impulse entrainment is determined using a systems analysis procedure. This method appears to be very sensitive to such variations. Threshold potential variations do not appear to be a primary determinant of the impulse frequency generated by a tonic neuron. This follows from a comparison of model and neural dynamics which indicates that accommodative changes in the neural threshold potential are small, and impulse initiated refractoriness relaxes on a time scale that is short compared to the interspike intervals. The nature of the small accommodative threshold variations, which are correlated with the action of sodium channel inactivation as well as potassium channel kinetics, suggests that the sodium channel is equally important in the control of the membrane potential during the greater part of the interspike interval following the immediate post spike undershoot.

1. Introduction

Transient elevations in the threshold for nerve impulse initiation are manifest in both accommodation to depolarizing stimulus currents, as well as in the refractoriness following impulses. Such threshold variations are therefore an implicit feature during the generation of impulse trains. As the excitability state of the nerve membrane varies during repetitive firing the instantaneous threshold can be defined in terms of the amplitude of a brief, depolarizing current pulse that will generate an action potential without further stimulus in 50% of trials. In the limit of an infinitesimally short time period for current pulse application the threshold stimulus becomes a quantity of charge whose effect, when applied, is to depolarize the membrane capacitance. Thus the instantaneous threshold may be defined in terms of the corresponding level of membrane depolarization.

* Supported by NSF grant BNS 77-22532. Computer facilities were made available through a grant from the University of Minnesota Computer Center.

The specific question to be addressed is the relative importance of variations of threshold as a part of the strategy employed by tonic neurons in determining the impulse spacing to given stimuli. Repetitive firing has been modelled for a considerable period of time with the contemporary notions about excitation serving as the underlying mechanism (c.f. Adrian (1928) and Katz (1939) for early models). Following the description of the action potential by Hodgkin and Huxley (1952) in terms of ion-specific conductance changes, many attempts have been made to describe the *sequencing* of impulses in terms of these mechanisms. Thus the spacing of impulses during low frequency repetitive firing has been described in terms of the action of slowly varying, voltage-gated potassium channels (Kernell and Sjöholm, 1972) as well as in terms of models containing only 'fast' conductance changes (Connor, 1978). It has been described in terms of neuron geometry (Traub and Llinás, 1977), and therefore in terms of effects that depend on the non-space-clamped environment of the excitable neural membrane (Fohlmeister, 1980). It has further been described in terms of the action of an electrogenic Na-K pump (Sokolove and Cooke, 1971) as well as in terms of a variable impulse threshold (Hartline, 1976). Each of these mechanisms acting as a part of, or in conjunction with, standard membrane excitation kinetics has been shown to be capable of both generating low frequency impulse trains and endowing them with a certain frequency stability (i.e. the impulse frequency is not an overly sensitive function of very small differences in stimulus). In one instance, a special case in which the spheroidal cell body itself acts as impulse trigger zone, the dominant mechanism consisting of a second, slowly varying potassium channel was determined by direct voltage clamp methods (Connor and Stevens, 1971).

However, the tonic repetitive firing of many peripheral neurons has led to a problem; the dominant mechanism for impulse entrainment is not at all obvious from any direct observation. The repetitive firing which is triggered on the initial segment or axon hillock has not been accessible to the voltage clamp technique, and the neural geometry is complex. The difficulty of this situation is compounded by the observation, using extracellular stimulus techniques, that the repetitive excitation properties at the impulse trigger zone do not match those of the typical axonal membrane which is usually phasic (Grampp, 1966; Nakagima and Onodera, 1968; Ringham, 1971). Because of this situation, methods of analysis of the spike train itself have been devised in attempts to make the discrimination. Models that emphasize one or another putative mechanism are constructed and subjected to spike train analysis for the purpose of evaluating the neural data.

Three neuron models are used in the evaluation of threshold phenomena. Two of these, the linear and leaky integrators are used to test for model independence of the results without the need to deal with the complicating effects of excitable channel kinetics. The third model, the 'variable- γ ' model contains a voltage-gated and time-dependent potassium channel and was generally constructed to closely reproduce the behavior of repetitively firing neurons in the interspike interval (Figure 1, and Fohlmeister *et al.*, 1974).

The absence of a regenerative (sodium) channel in all of these models prevents

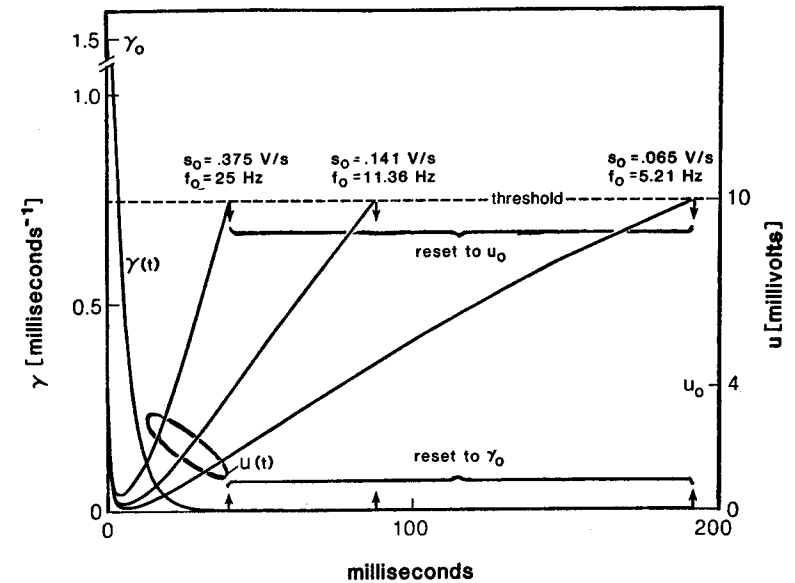


Fig. 1. Membrane potential (u) trajectories and $\gamma(t)$ trajectories generated by the variable- γ model for three different lengths of interspike interval. Upon reaching threshold potential ($\theta = 10$ mV) an impulse is assumed to occur and the variables are reset to $u_0 = 4$ mV and $\gamma_0 = 1.48$ ms $^{-1}$. $B = 0.2$ ms $^{-1}$ and $D = 5 \times 10^{-5}$ ms $^{-2}$ mV $^{-1}$.

them from generating simulated impulses. This property allows variable threshold conditions to be imposed and evaluated. Impulses are assumed to occur whenever a well defined threshold is reached. The models, including both accommodative and impulse initiated threshold variations are subjected to a systems analysis procedure (dynamic analysis, see Section 2) and the outcome is compared with similar data from the tonic abdominal stretch receptor neuron of the crayfish.

2. Methods

General outline of dynamic analysis

The procedure to which the models and neurons are subjected consists of linear combinations of two stimulus currents

$$(1) \quad i(t) = i_0 + i_1 \sin(\omega t)$$

(injected intracellularly in the case of the crayfish neuron) where i_0 is a constant level of depolarizing current perturbed by a small amplitude sinusoidal current of amplitude $|i_1|$ and angular frequency ω . i_0 establishes a steady state frequency, f_0 , of impulses in tonic neurons; f_0 is called the 'operating point' herein. The sinusoidal component of the stimulus causes a perturbation of the impulse frequency

(pulse frequency modulation) about the operating point. The raw response data consist of records of the times, t_{imp} , of impulse occurrence. These times are converted modulo $2\pi/\omega$

$$(2) \quad t = t_{\text{imp}}(\text{mod } 2\pi/\omega)$$

so that they fall within the interval of one period, $2\pi/\omega$, of the stimulus sine wave. Expressed another way, the repeating periods of the stimulus sine wave are overlaid with the times of impulse occurrence clearly marked (see Fohlmeister *et al.*, 1980, Figure 2). For this purpose, each occurrence of a given, fixed phase of the perturbing sine wave was recorded in the raw temporal data (sync. pulses). All times were determined to within ± 0.05 ms.

There are $2\pi f_0/\omega$ impulses per perturbation period on the average, but the impulses are not distributed with equal likelihood throughout the interval of the period. Thus the *impulse density* within the overlaid interval will vary sinusoidally with the period of the perturbation stimulus provided that the amplitude $|i_1|$ is sufficiently small to prevent non-linear distortions of the impulse density function (*ibid.*). Gain and phase of the impulse density function are then determined relative to the stimulus perturbation sine wave (Knight, 1972; Fohlmeister *et al.*, 1977a). For a given model or neuron these quantities are functions only of the operating point f_0 , and of ω . The gain and phase data are plotted as functions of $\omega/2\pi f_0$ (Bode plots).

Because most of the existing neural dynamics data cover a range of ω extending two orders of magnitude below an upper limit of $2\pi f_0$, we restrict our Bode plots to this range (see Figures 2-9). In evaluating the relevant phenomena, it is convenient to speak of the upper, middle and lower thirds of this range. The upper third is dominated by a resonance in gain as $\omega \rightarrow 2\pi f_0$. The accommodative threshold variations (introduced below) have a direct effect on the width of this gain resonance in addition to the associated phase changes (Fohlmeister *et al.*, 1974). On the other hand, impulse initiated threshold elevations behave dynamically like inhibitory feedback, one form of which produces a midrange gain enhancement with an antisymmetric (about $\omega/\pi f_0$) distortion of the phase (Fohlmeister *et al.*, 1977a, Figure 7).

Neuron models

Three models for the control of the membrane potential trajectory in the interspike intervals are subjected to dynamic analysis. The form of the differential equation for the membrane potential, $u \equiv E - E_K$, in the interspike intervals is the same for each model:

$$(3) \quad \frac{du}{dt} = -\frac{g_K}{C}u + \frac{i}{C} \equiv -\gamma u + s.$$

The membrane potential is referenced to the potassium equilibrium potential, E_K , under the assumption that the K-conductance plays a dominant role in the

interval between impulses. Each of the models postulates that an impulse occurs whenever u reaches a predetermined, positive threshold value, which in turn resets u to a smaller positive value near the ordinary membrane resting potential. Therefore, when stimulated with a suprathreshold current i (or s) the systems operate like relaxation oscillators. The dynamics are insensitive to the levels of *mean* threshold and reset value of u chosen for spike train simulations.

The simplest of the three models, the linear integrator assumes $\gamma = 0$. A constant current, i or s , leads to a linear ramp trajectory for the membrane potential in the interspike interval and a sawtooth pattern during repetitive firing. In contrast, the leaky integrator with a non-zero, positive and constant γ leads to interspike trajectories of exponential form. Its dynamics are fundamentally different from those of the linear integrator, and consist of a resonance in the gain as $\omega/2\pi \rightarrow f_0$ with a simultaneous phase advance in the upper third of the dynamic range (c.f. Figures 6 and 7; the linear integrator's gain and phase are flat with phase = 0). It follows that the dynamics are sensitive to the presence of a resistive path (membrane conductance) for the membrane current (c.f. the dynamics of the variable $-\gamma$ model below).

The third, and most complex of the models, the variable $-\gamma$ model makes γ into a second state variable following the equation

$$(4) \quad \frac{d\gamma}{dt} = -B\gamma + Du,$$

where B and D are constants, with initial condition, γ_0 , at the beginning of each interspike interval. The values of $\gamma_0 = 1.48 \text{ ms}^{-1}$, $B = 0.2 \text{ ms}^{-1}$, and $D = 5 \times 10^{-5} \text{ mV}^{-1} \text{ ms}^{-2}$ are so chosen that the resulting potential (u) trajectory follows that of the tonic neurons including the post-spike undershoots (see Figure 1). Fine 'tuning' of the parameters was done to achieve maximum agreement with neural dynamics. The dynamics of this model are related to those of the leaky integrator and include a gain resonance and upper range phase advance. However, the phase advance is much less pronounced for the variable $-\gamma$ model and agrees with the tonic neurons in this respect (Fohlmeister *et al.*, 1974).

Dynamics of threshold potential variations

The degrees of mathematical complexity of the three models are such that analytic expressions for gain(ω) and phase(ω) can be derived for only the linear and leaky integrators ($\gamma = \text{constant}$, see equations (12), (13) and (14)). The method used is that of perturbation theory wherein zero-order, steady-state values (constant stimulus s_0 , constant threshold θ_0 , and constant impulse frequency f_0) are perturbed by the stimulus sinusoid ($i_1 \sin(\omega t)$ in equation (1)). The transfer function is calculated to first order. The perturbation technique has been described in Fohlmeister *et al.* (1974, 1977a,b).

Threshold θ , stimulus s , and the parameter γ are related to the interspike period T by the following integral (Knight, 1969).

$$(5) \quad \theta = \int_0^T s e^{-(T-t)\gamma} dt.$$

If we assume that the threshold potential is abruptly increased by an amount, Δ , above the preimpulse value whenever an impulse occurs and then declines exponentially with time constant, τ , to a baseline of θ_0 then we have in the steady state

$$(6) \quad \left(\Delta \sum_{l=0}^{\infty} e^{-lT_0/\tau} \right) e^{-T_0/\tau} + \theta_0 = \int_0^{T_0} s_0 e^{-(T_0-t)\gamma} dt$$

where the sum over l is the residual effect of all previous impulse initiated threshold elevations (accumulating impulse initiated threshold elevations). Since the sum of the infinite series is

$$(7) \quad \sum_{l=0}^{\infty} e^{-lT_0/\tau} = 1/(1 - e^{-T_0/\tau})$$

we define

$$(8) \quad \hat{\Delta} \equiv \Delta/(e^{T_0/\tau} - 1)$$

and equation (6) becomes

$$(9) \quad \hat{\Delta} + \theta_0 = s_0 \int_0^{T_0} e^{-(T_0-t)\gamma} dt$$

in the steady state with accumulating threshold elevations.

On the other hand, if impulse occurrence resets threshold to a fixed value (non-accumulating) then

$$(10) \quad \Delta_{na} e^{-T_0/\tau} + \theta_0 = s_0 \int_0^{T_0} e^{-(T_0-t)\gamma} dt$$

for which a steady state is reached after the first impulse. In this case Δ_{na} is the fixed threshold increment above the baseline θ_0 .

With the introduction of the perturbation stimulus current (corresponding to the i_1 term in equation (1)) an *accommodating* threshold variation, θ_1 , may be introduced so that equation (5) becomes

$$(11) \quad \left(\Delta \sum_{l=0}^{\infty} \exp[-\hat{T}(l, \omega, T_0)/\tau] \right) e^{-T/\tau} + \theta_0 + \theta_1 e^{i\omega t} = \int_0^T (s_0 + s_1 e^{i\omega t}) e^{-(T-t)\gamma} dt$$

where

$$(11A) \quad \hat{T}(l, \omega, T_0) = lT_0 + T_1 \frac{1 - \exp(-i\omega T_0)}{\exp(i\omega T_0) - 1}$$

to first order perturbation theory (Fohlmeister, 1979, Appendix). Note that lT_0 in the infinite series of equation (6) becomes \hat{T} in equation (11) because the length of preceding interspike periods is now modulated to the extent of the T_1 term. All quantities with subscript 1 are perturbation terms and are therefore assumed to be a small fraction (in magnitude) of the corresponding steady state terms with subscript 0. This condition can always be arranged experimentally by choosing a sufficiently small perturbation stimulus amplitude $|s_1|$.

The sinusoidal perturbation is entered as a complex exponential in equation (11) so that the two real quantities of gain(ω) and phase(ω) are derived from a complex transfer function. Perturbation quantities with subscript 1 are therefore complex numbers.

For the leaky (and linear) integrator models the transfer function $F(i\omega)$ is given by

$$(12) \quad \frac{f_0}{s_0} F(i\omega) \equiv \frac{f_1}{s_1} = \frac{f_0}{s_0} \left[1 + \left(\frac{\hat{\Delta}}{\tau s_0} \right) \frac{\exp(\gamma/f_0)}{1 - \exp[-(1/\tau + i\omega)/f_0]} \right]^{-1} \times \\ \times \left(\frac{i\omega}{i\omega + \gamma} \right) \frac{1 - [1 - (\theta_1/s_1)(i\omega + \gamma)] \exp[(i\omega + \gamma)/f_0]}{1 - \exp(i\omega/f_0)}$$

in terms of which

$$(13) \quad \text{gain}(\omega) \equiv 20 \log |F(i\omega)|,$$

and

$$(14) \quad \text{phase}(\omega) \equiv \tan^{-1} \frac{\text{Im}F(i\omega)}{\text{Re}F(i\omega)}$$

f_1 of equation (12) is related to T_1 by

$$(15) \quad f_0 + f_1 \left(\frac{1 - \exp(i\omega/f_0)}{-i\omega/f_0} \right) = \frac{1}{T_0 + T_1} = \frac{1}{T_0} - \frac{T_1}{T_0^2} + O(T_1^2)$$

so that

$$(16) \quad f_0 \approx 1/T_0,$$

and

$$(17) \quad f_1 = T_1 f_0^2 \left(\frac{i\omega/f_0}{1 - \exp(i\omega/f_0)} \right).$$

The definition of f_1 is such that its magnitude $|f_1|$ gives the amplitude of the sinusoidal variation of the impulse density. Its argument ϕ

$$(18) \quad f_1 = |f_1| e^{i\phi}$$

is such that the phase of the transfer function $F(i\omega)$ given by equation (14) represents the phase difference between the impulse density sinusoid (the output) and the stimulus perturbation sinusoid (the input). The factor $(i\omega/f_0)/[1 - \exp(i\omega/f_0)]$ is due to the conversion to impulse density by the use of equation (2); the continuous frequency variations of a single neuron [represented by the T_1 term in equation (11A)] are viewed as the population response of an ensemble of identical neurons over one perturbation period (c.f. Knight, 1972). None of the conclusions of this paper are affected by this frequency dependent factor which is included because impulse density is intuitively a more meaningful output function.

The derivation of the transfer function (12) follows standard lines (e.g. Fohlmeister, 1979, Appendix). Note that phase angles introduced between θ_1 and s_1 represent time delays between the stimulus perturbation and the resulting accommodative threshold responses.

The complexity of the variable- γ model precludes a derivation of analytic forms for $\text{gain}(\omega)$ and $\text{phase}(\omega)$, and the equations were integrated numerically (Runge-Kutta routine on the Control Data Corporation Cyber 74 computer at the University of Minnesota Computer Center) to determine the perturbed impulse trains. The stimulus perturbation amplitude $|s_1| = 0.1s_0$ for all integrations. The impulse trains were then subjected to the same procedure as the tonic neuron impulse trains for $\text{gain}(\omega)$ and $\text{phase}(\omega)$ extraction (c.f. subsection: General outline of dynamic analysis).

3. Results

Threshold dynamics for a fixed operating point

Accommodative threshold variations.—The principal dynamic effects of accommodative threshold variations (denoted by a nonzero θ_1 in the previous section) are to *increase* the gain resonance width and to *retard* the upper range phase. Although this general feature holds for all three types of model considered herein it is demonstrated most clearly with the linear integrator in Figure 2 for which the gain and phase are flat as functions of ω when threshold is constant. Figure 3 shows the effect for the variable- γ model. The curves of Figure 2 were analytically derived from first order perturbation theory; those of Figure 3 are the gain and phase determined from computer generated spike trains which were then treated like actual neural spike trains.

Impulse initiated threshold elevations.—The principal dynamic effects of impulse initiated threshold variations are given in Figure 4, in this case for the leaky integrator with accumulative (summing) threshold elevations (denoted by Δ in the previous section). Again, the midrange gain enhancement, symmetrical about $\omega = \pi f_0$, and the antisymmetric (about $\omega = \pi f_0$) phase variations are common to the three model types. Figure 4 shows the normal leaky integrator dynamics as dashed curves with which the symmetrical gain component is algebraically summed and the phase antisymmetrically distorted. (These symmetrical and antisymmetric features alone are plotted on a linear frequency scale in Fohlmeister *et al.* (1977a),

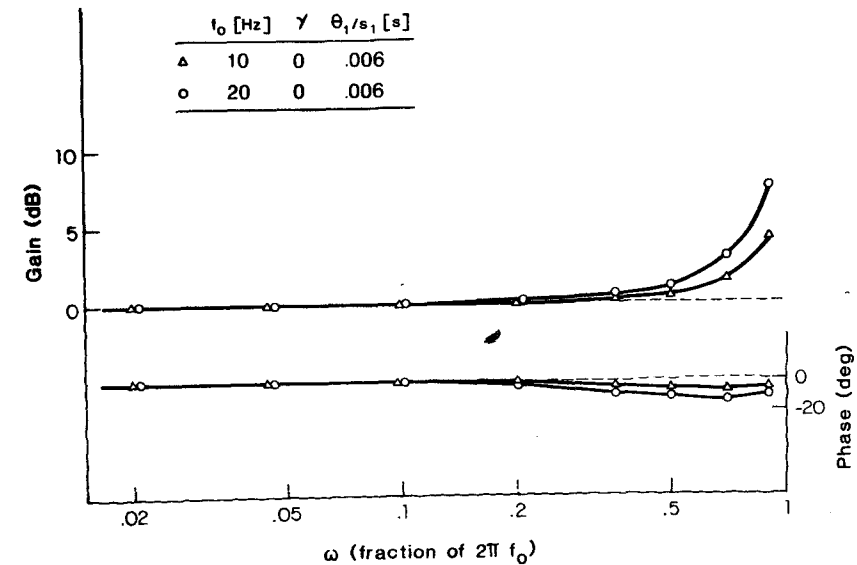


Fig. 2. Gain and phase as functions of the perturbation frequency generated by the linear integrator model ($\gamma = 0$) with accommodating threshold variations. Gain and phase are flat (---) for this model with $\theta_1 = 0$.

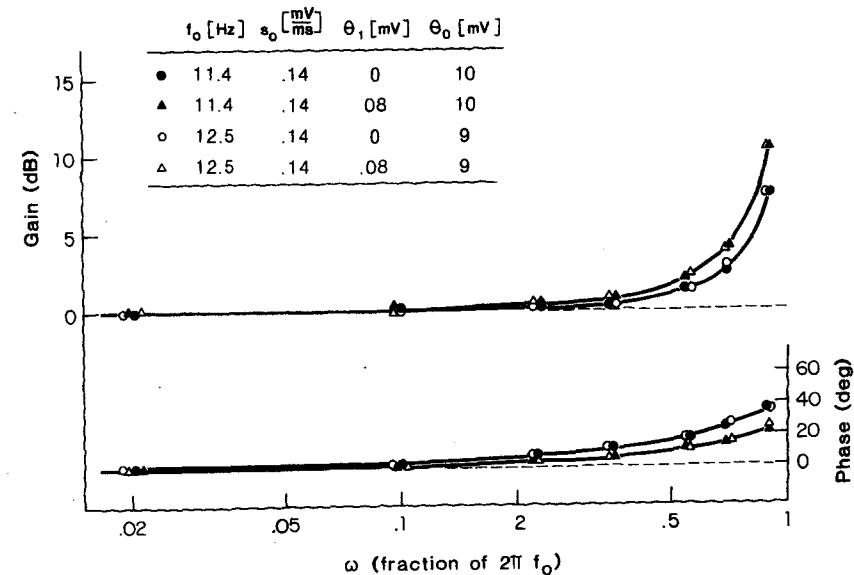


Fig. 3. Gain and phase generated by the variable- γ model with (Δ) and without (\circ) accommodating variations in threshold potential.

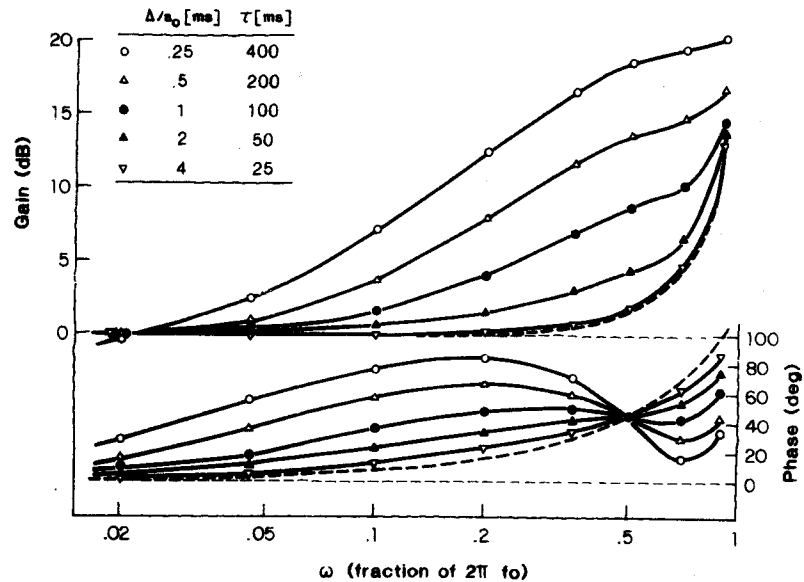


Fig. 4. Gain and phase generated by the leaky integrator model in the presence of accumulating impulse initiated threshold elevations. $\gamma = 32 \text{ s}^{-1}$ and $f_0 = 10 \text{ imp/s}$. Note that the curves approach the leaky integrator gain and phase (dashed curves) as the time constant, τ , for threshold relaxation shortens even though the magnitude of the spike initiated threshold elevation, Δ/s_0 , is increased proportionately. This behavior is expected since the effects of accumulating and non-accumulating threshold elevations become identical when the elevations decay rapidly.

Figure 7.) Figure 5 shows the same phenomenon for the variable- γ model for which data points are plotted for both accumulating and non-accumulating impulse initiated threshold elevations. Note that the non-accumulating threshold is not recognized in the dynamics and leads to gain and phase curves like those with no threshold variations at all. The dynamic behavior of accumulating and non-accumulating threshold elevations is in fact identical to that of accumulating and non-accumulating inhibitory feedback respectively (see Fohlmeister *et al.* (1977a) for a detailed discussion of the dynamics of the latter two and their interaction).

Dynamics as a function of the operating point, f_0 ; accommodative threshold variations

Leaky integrator with $\gamma/f_0 = \text{constant}$.—Figure 6 shows the behavior of the dynamics for the leaky integrator in the presence of accommodative threshold variations when the unmodulated impulse frequency (the operating point, f_0) is increased. The gain resonance width increases with increasing f_0 . When $\theta_1 = 0$, the resonance width is independent of f_0 for the values of the parameter γ chosen

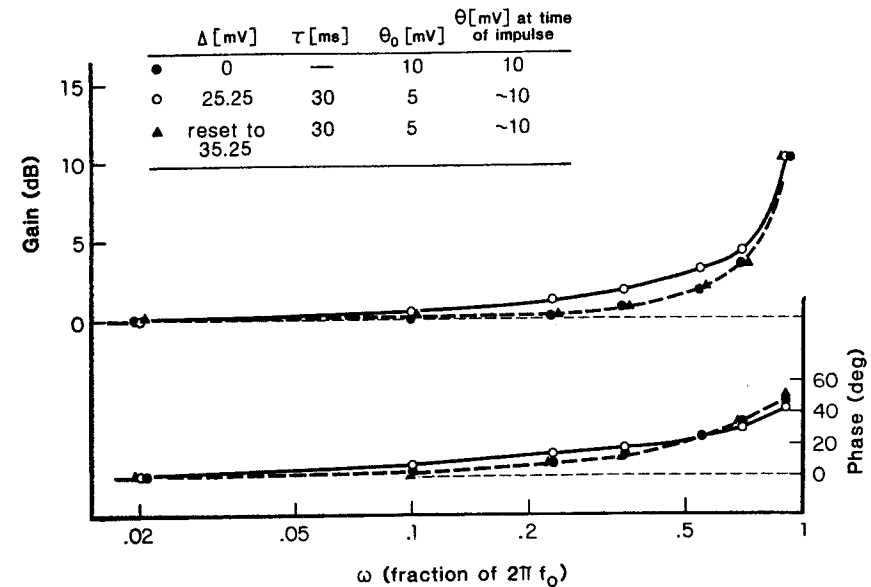


Fig. 5. Gain and phase generated by the variable- γ model in the absence of threshold variations (●, $\theta_1 = 0$) as well as in the presence of non-accumulating (△) and accumulating (○) impulse initiated threshold elevations. $f_0 = 18.5 \text{ imp/s}$ and $s_0 = 0.25 \text{ mV/ms}$. Parameters were adjusted so that the threshold at the time of impulse occurrence for an unperturbed steady state impulse train was $\theta \approx 10 \text{ mV}$ for all three cases. However, this is not a necessary condition, and the dynamics are very nearly the same even if this condition is violated by the choice of other values of θ_0 .

in the figure. These γ values are such that $\gamma/f_0 = \text{constant}$. Equation (12) shows that the dynamics are invariant when γ/f_0 is held constant and when all threshold variation terms are zero.

Figure 6 shows further that the upper range phase advance decreases as f_0 increases for a non-zero θ_1 and for $\gamma/f_0 = \text{constant}$. When $\theta_1 = 0$, the phase advance remains independent of f_0 for the reason given above (c.f. equations (12) and (14)).

Leaky integrator with $\gamma = \text{constant}$.—When γ is held fixed and f_0 is increased the corresponding dynamics are shown in Figure 7. Note that the gain resonances tend to cluster somewhat in this case with the width first decreasing ($f_0 = 7 \rightarrow 14 \text{ Hz}$) and then increasing slightly ($f_0 = 14 \rightarrow 20 \text{ Hz}$). At the same time the phase advance becomes strongly dependent on the operating point, f_0 . The increased functional dependence of the phase in Figure 7 over that in Figure 6 is due to the declining value of the ratio γ/f_0 as f_0 increases in Figure 7. The abscissa scale, $\omega/2\pi f_0$, was so chosen that operating points overlap in Figures 6 and 7 and all subsequent figures (as well as in Figure 2). This allows ready observation of

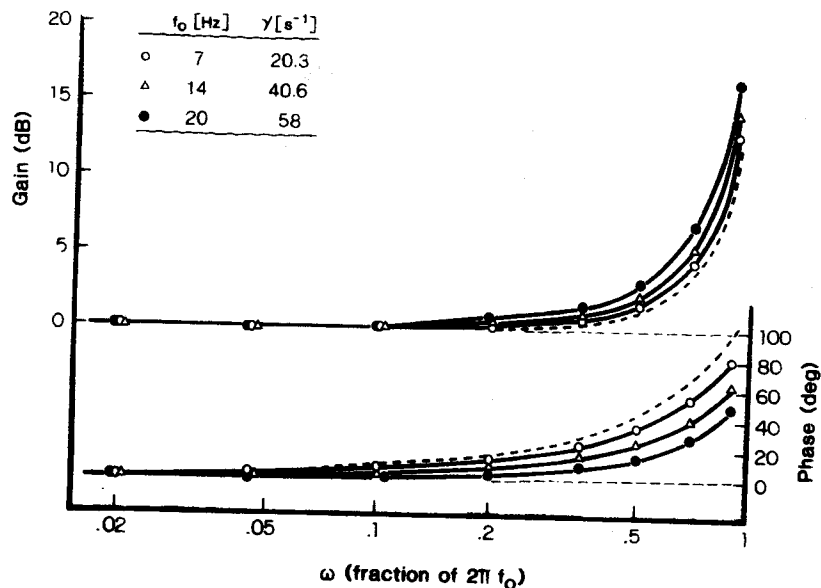


Fig. 6. Gain and phase of the leaky integrator with accommodating threshold variations, $\theta_1/s_1 = 0.006$ s. Dashed curves give the dynamics of the leaky integrator model with $\theta_1 = 0$. The ratio $\gamma/f_0 = 2.9 = \text{constant}$ for all curves.

'dynamic movement' with respect to the $\gamma/f_0 = \text{constant}$ feature (c.f. equation (12)). For the neurons both gain and phase are relatively weakly dependent on f_0 on such a plot (Figure 7, neural data).

Variable- γ model and delayed accommodation.—The variable- γ model in the presence of accommodative threshold variations shows the usual gain resonance enhancement and phase reduction when f_0 is held constant (Figure 3). However, as a function of the operating point both the gain width and the phase advance tend to increase somewhat with increasing f_0 (Figure 8). A small increase in both quantities is a property of the variable- γ model even in the absence of threshold variations. However, Figure 9 shows that this trend is reversed for the gain when a time lag (of 4 ms) is introduced in the threshold response relative to the stimulus perturbation. Furthermore, the phase curves, for which the trend is not reversed, tend to straighten somewhat as $\omega \rightarrow 2\pi f_0$ under this condition. Both features are observed in the data of typical neurons (Figure 7). The small increase in the upper ω range phase advance with increasing f_0 is also consistent with the neural data when those data are corrected for the electrotonic delay due to the neural cable properties between the stimulus application at the micropipette tip in the soma and its effect at the impulse trigger zone (Fohlmeister *et al.*, 1977b).

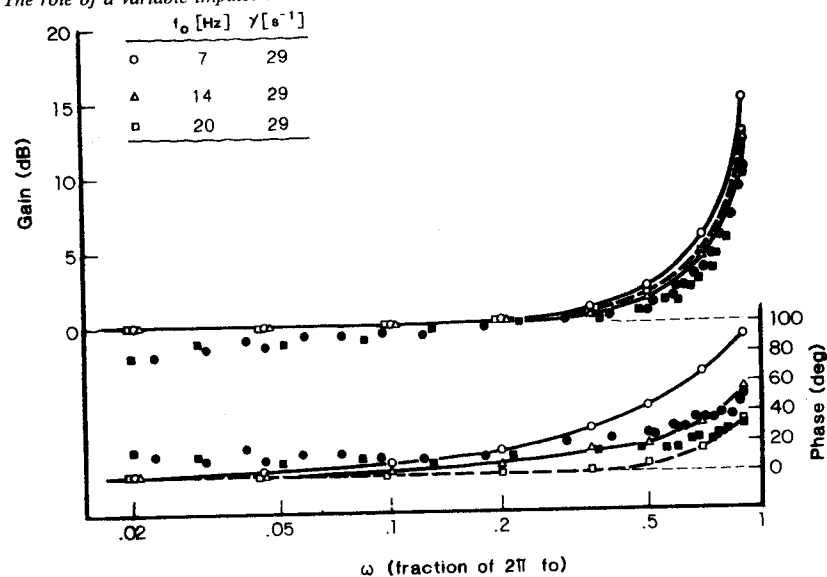


Fig. 7. Gain and phase of the leaky integrator with accommodating threshold variations, $\theta_1/s_1 = 0.006$ s, and $\gamma = 29$ s^{-1} held fixed for all curves. Filled data points are from the crayfish receptor neuron for $f_0 = 8$ to 10 imp/s (●) and $f_0 = 19.1$ to 22 imp/s (■). The lower range gain depression and phase advance is due to the summing inhibitory (negative) feedback effect of an electrogenic Na-K pump (Fohlmeister *et al.*, 1977b). Data redrawn from Fohlmeister *et al.* (1974, 1977b).

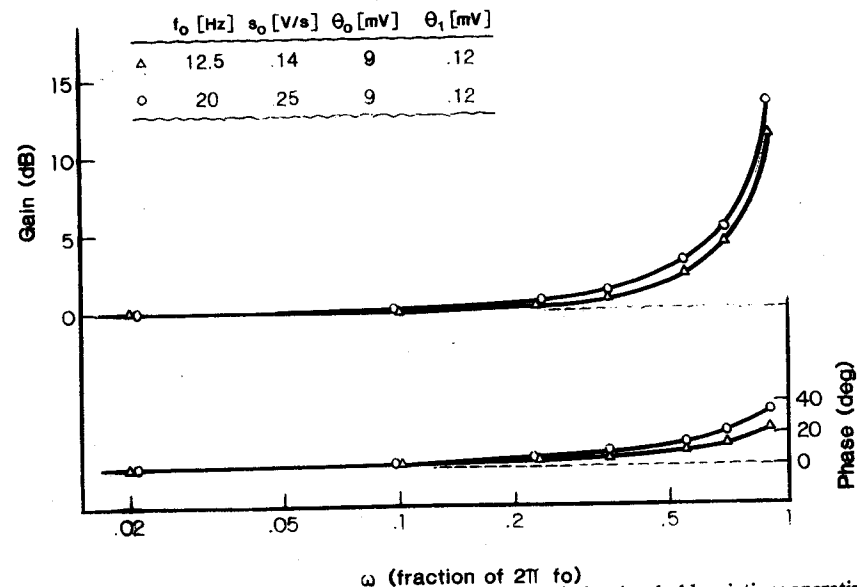


Fig. 8. Gain and phase of the variable- γ model with accommodating threshold variations operating at two impulse frequencies f_0 .

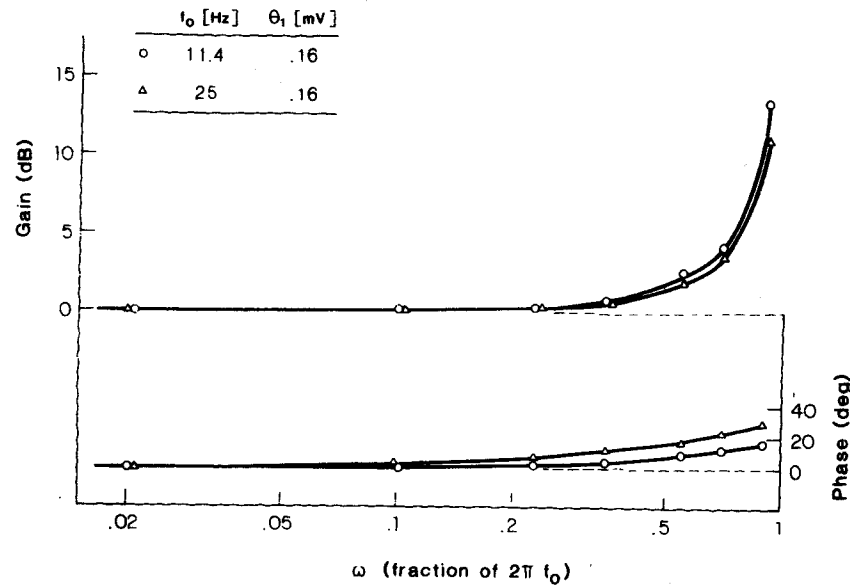


Fig. 9. Gain and phase at two operating points f_0 of the variable- γ model with accommodating threshold variations and a fixed time delay (4 ms) in the phase of the threshold response relative to the stimulus perturbation.

4. Conclusions and discussion

Dynamic analysis of nerve models appears to be extremely sensitive to both accommodative and accumulating impulse initiated variations in threshold potential. This follows from the relatively large observed effects in gain and phase when very small variations in threshold potential are assumed for the models (c.f. the values of θ_1 in Figures 3 and 8). On the other hand, threshold potential variations that are impulse initiated and that do not accumulate from interval to interval are not recognized in the dynamics (Figure 5). Therefore, a comparison of model and neural dynamics data shows that:

- (1) accommodative threshold potential variations appear to be present to a very limited degree during low frequency repetitive firing of the tonic stretch receptor neuron of the crayfish (c.f. also Eyzaguirre and Kuffler, 1955); and
- (2) impulse initiated elevations in threshold appear to be reset with the occurrence of the next impulse; that is, there is virtually no memory of the earlier states of excitation following the occurrence of an impulse.

However, note in Figure 4 that the dynamic characteristics of accumulating threshold elevations tend to disappear when such elevations relax with a short

time constant. The lack of memory may therefore be due to the rapid relaxation of the effect rather than its eradication by the next impulse.

A third conclusion is that models based primarily on a variable threshold to reproduce the tonic repetitive firing of neurons will not satisfy neural dynamics. This follows from the argument that impulse initiated threshold elevations in conjunction with the leaky or linear integrator models either do not modify the dynamics (non-accumulating) or they generate an inappropriate dynamic response (accumulating threshold elevations) when compared with the neurons. Accommodating threshold variations can be adjusted so that the gains of the leaky integrator and neurons are similar. However, the leaky integrator phase then becomes strongly dependent on f_0 which is contrary to the neural phase (Figure 7).

On the other hand, certain threshold phenomena appear to correct small deficiencies in the dynamics of models that are primarily based on restricted conductance kinetics, such as the variable- γ model. Conductance kinetics were introduced as the next step following the leaky integrator model in order to satisfy the crayfish neural dynamics (Fohlmeister *et al.*, 1974). The neural gain resonance width decreases slightly with increasing f_0 , whereas the width generated by the variable- γ model tends to increase slightly when f_0 is increased and the threshold potential is held constant. This behavior of the variable- γ model is reversed in the presence of accommodating threshold variations provided a short time delay is introduced between the stimulus perturbation and the threshold response (Figure 9). An additional effect of the time delay is to straighten the upper range phase curve somewhat, an effect seen in most neural data.

The need to add an accommodative threshold effect to an otherwise discontinuous threshold model might be expected *a priori*. It recognizes the action of sodium channel inactivation (the h parameter of the Hodgkin and Huxley (1952) model is a steep function of voltage in the region between the resting and threshold potentials; that is in the vicinity of -60 mV) and possibly some potassium channel activation. Both tend to increase threshold and operate with time constants of the order of several milliseconds at these membrane potentials and the temperature (17°C) for which crayfish data were obtained. The time delay introduced into the accommodative threshold variations of the variable- γ model are consistent with these time constants.

The correlation of 'delayed accommodation' with sodium inactivation and potassium activation is consistent with further results of the dynamics. Figure 1 shows that the state variable γ is near zero during most of the interspike interval for low frequency repetitive firing. This is necessary for the model to generate neural dynamics. The nearness of γ to zero suggests that the action of the sodium channel may be important in most of the interspike interval. The state variable γ becomes more generally

$$C\gamma = g_K + g_{Na} \left(\frac{E - E_{Na}}{E - E_K} \right), \quad E > E_K$$

for a model system that includes both a sodium and a potassium channel. Note that the sodium (Na) term is negative for $E_K < E < E_{Na}$, which would tend to balance out (or cancel) a positive g_K .

With this (as well as other factors) in mind, models that include both a regenerative sodium and a potassium channel have been constructed following the lines of the Hodgkin-Huxley (1952) model parametrization but with modified rate constants (Fohlmeister, 1980). The dynamics of these models show that the sodium current must indeed be approximately equal in magnitude to the potassium current during most of the interspike interval in order to agree with the dynamics of the crayfish neuron. Since during repetitive firing the membrane potential is monotonically increasing following the after-hyperpolarization in the interspike interval (discounting rapid fluctuations of electrical noise), both sodium inactivation and potassium activation must act to prevent the sodium activation from reaching regenerative proportions too early. It is this action of the (recovery) variables h and n that may be correlated with the 'delayed accommodative' threshold effect in conjunction with the variable- γ model.

Finally, since the impulse entrainment occurs in a non-space clamped mode it is instructive to identify the neural component to which these arguments dealing with excitable channel gating and threshold potential apply. The output, namely the sequence of impulses, emanates from a trigger zone with little distortion of the impulse spacing on the way to the recording site. Therefore, one may argue that the results apply to the trigger zone membrane. This argument is strengthened by the observation that any distortion of the input at the trigger zone (the generator current, equation (1)) due to longitudinal currents associated with the back-propagation of impulses from the trigger zone to the electrode tip in the soma will act like impulse initiated feedback. The absence in the neural dynamic data of an unidentified feedback effect supports the conclusion that such input distortions can be ignored.

However, the impulses are not initiated on a space-clamped piece of membrane, and subthreshold electrical communication of the trigger membrane with neighboring membrane also leads to longitudinal currents. Any excess charge on the membrane surface such as that due to a stimulus current pulse will not be dissipated through the local membrane channels alone as in the case of a space clamped membrane. The situation is as though there were another current path in parallel with those of the membrane channels of the actual trigger patch of membrane whose properties will influence the threshold condition in conjunction with the kinetic properties of the membrane channels (Fohlmeister, 1980). Thus the instantaneous threshold potential of the embedded trigger membrane may be different from that of space clamped trigger zone membrane alone. Due to the nature of spike train dynamic analysis it is the threshold potential of the *in situ* trigger membrane, whose variations are considered herein.

References

- Adrian, E. D. (1928). *The basis of sensation. The action of sense organs*. Cristofers, London.
- Connor, J. A. (1978). Slow repetitive activity from fast conductance changes in neurons. *Federation Proc.* **47**, 2139-2145.
- Connor, J. A. and Stevens, C. F. (1971). Prediction of repetitive firing behavior from voltage clamp data on isolated neuron soma. *J. Physiol.* **213**, 31-53.
- Eyzaguirre, C. and Kuffler, S. W. (1955). Processes of excitation in the dendrites and in the soma of single isolated sensory nerve cells of the lobster and crayfish. *J. Gen. Physiol.* **39**, 87-119.
- Fohlmeister, J. F. (1979). A theoretical study of neural adaptation and transient responses due to inhibitory feedback. *Bull. Math. Biol.* **41**, 257-282.
- Fohlmeister, J. F. (1980). Electrical processes involved in the encoding of nerve impulses. *Biol. Cybernetics* **36**, 103-108.
- Fohlmeister, J. F., Adelman, W. J. and Poppele, R. E. (1980). Excitation properties of the squid axon membrane and model systems with current stimulation: statistical evaluation and comparison. *Biophys. J.* **30**, 79-98.
- Fohlmeister, J. F., Poppele, R. E. and Purple, R. L. (1974). Repetitive firing: dynamic behavior of sensory neurons reconciled with a quantitative model. *J. Neurophysiol.* **37**, 1213-1227.
- Fohlmeister, J. F., Poppele, R. E. and Purple, R. L. (1977a). Repetitive firing: a quantitative study of feedback in model encoders. *J. Gen. Physiol.* **69**, 815-848.
- Fohlmeister, J. F., Poppele, R. E. and Purple, R. L. (1977b). Repetitive firing: quantitative analysis of encoder behaviour of slowly adapting stretch receptor of crayfish and eccentric cell of *Limulus*. *J. Gen. Physiol.* **69**, 849-877.
- Grampp, W. (1966). The impulse activity in different parts of the slowly adapting stretch receptor neuron of the lobster. *Acta Physiol. Scand.* **66**, 1-36.
- Hartline, D. K. (1976). Simulation of phase-dependent pattern changes in perturbations of regular firing in crayfish stretch receptor. *Brain Research* **110**, 245-257.
- Hodgkin, A. L. and Huxley, A. F. (1952). A quantitative description of membrane current and its application to conduction and excitation in nerve. *J. Physiol.* **117**, 500-544.
- Katz, B. (1939). *Electrical Excitation of Nerve: A Review*. Oxford University Press, London.
- Kernell, D. and Sjöholm, H. (1972). Motoneurone models based on 'voltage clamp equations' for peripheral nerve. *Acta Physiol. Scand.* **86**, 546-562.
- Knight, B. W. (1969). Frequency response for sampling integrator and for voltage to frequency converter. In: *Systems Analysis in Neurophysiology* (Terzuolo, C. A., Ed.). University of Minnesota Press, Minneapolis.
- Knight, B. W. (1972). Dynamics of encoding in a population of neurons. *J. Gen. Physiol.* **59**, 734-766.
- Nakagima, S. and Onodera, K. (1969). Membrane properties of the stretch receptor neurons of crayfish with particular references to mechanisms of sensory adaptation. *J. Physiol.* **200**, 161-185.
- Ringham, G. L. (1971). Origin of nerve impulse in slowly adapting stretch receptor of crayfish. *J. Neurophysiol.* **34**, 773-784.
- Sokolove, P. G. and Cooke, J. M. (1971). Inhibition of impulse activity in a sensory neuron by an electrogenic pump. *J. Gen. Physiol.* **57**, 125-163.
- Traub, R. D. and Llinas, R. (1977). The spatial distribution of ionic conductances in normal and axotomized motoneurons. *Neuroscience* **2**, 829-849.